

Light scalar WIMP through the Higgs portal and CoGeNTSarah Andreas,¹ Chiara Arina,² Thomas Hambye,² Fu-Sin Ling,^{2,3} and Michel H. G. Tytgat²¹*Deutsches Elektronen Synchrotron, Notkestrasse 85, D-22603 Hamburg, Germany*²*Service de Physique Théorique, Université Libre de Bruxelles, CP225, Bld du Triomphe, 1050 Brussels, Belgium*³*Institute for Particle Physics Phenomenology, Durham University, Durham, DH1 3LE, United Kingdom*

(Received 16 March 2010; revised manuscript received 21 July 2010; published 19 August 2010)

If dark matter (DM) simply consists in a scalar particle interacting dominantly with the Higgs boson, the ratio of its annihilation cross section—which is relevant both for the relic abundance and indirect detection—and its spin-independent scattering cross section on nuclei depends only on the DM mass. It is an intriguing result that, fixing the mass and direct detection rate to fit the annual modulation observed by the DAMA experiment, one obtains a relic density in perfect agreement with its observed value. In this article we update this result and confront the model to the recent CoGeNT data, tentatively interpreting the excess of events in the recoil energy spectrum as being due to DM. CoGeNT, as DAMA, points toward a light DM candidate, with somewhat different (but not necessarily incompatible) masses and cross sections. For the CoGeNT region too, we find an intriguing agreement between the scalar DM relic density and direct detection constraints. We give the 1σ region favored by the CDMS-II events, and our exclusion limits for the Xenon10 (2009) and Xenon100 data, which, depending on the scintillation efficiency, may exclude CoGeNT and DAMA. Assuming CoGeNT and/or DAMA to be due to scalar singlet DM leads to definite predictions regarding indirect detection and at colliders. We specifically emphasize the limit on the model that might be set by the current Fermi-LAT data on dwarf galaxies, and the implications for the search for the Higgs at the LHC.

DOI: [10.1103/PhysRevD.82.043522](https://doi.org/10.1103/PhysRevD.82.043522)

PACS numbers: 95.35.+d

I. INTRODUCTION

Recently, there has been some effervescence regarding what may be first hints of direct detection of dark matter (DM) from the galactic halo. The most recent hint is related to the CoGeNT experiment, a low background germanium crystal based detector, with a rather modest exposure time and detector mass, but very low threshold energy, which has announced an anomaly in the form of an excess of events at low recoil energies [1]. Although the collaboration clearly leans toward natural radioactivity as the cause for the observed excess (see also [2]), they do put forward the possibility that the events may be explained by the elastic collisions of DM from the galactic halo, with a mass in the $\sim 7\text{--}10\text{ GeV}$ range, and a rather large spin-independent (SI) cross section on nuclei, $\sigma_n^0 \sim 7 \times 10^{-41}\text{ cm}^2$.

Surprisingly, these values for the mass and scattering cross section are not too different from those required to fit the DAMA/Libra and DAMA/NaI (DAMA in the sequel) events. DAMA has observed 11 successive cycles of annual modulation in the rate of nuclear recoils, with a statistical significance of 8.2σ [3]. These measurements are consistent with the signal that would arise from elastic scattering of a WIMP from the galactic halo with the nuclei in the detectors, the flux of DM particles being modulated by the periodic motion of the Earth around the Sun [4,5].

There has been much work on the DM interpretation of the recent DAMA data (see e.g. [6–21]). In [22] (see also [23]), it has been shown that the DAMA results may be explained as being caused by the elastic scattering of a

singlet scalar DM candidate interacting through the Higgs portal. Note that such a particle may be a true singlet scalar [24–26], or the effective, low energy limit of a more sophisticated model.¹ Here we discuss the possible impact of new data, both from direct and indirect searches.

In Sec. II we first give the main properties of the singlet scalar dark matter candidate, S . There we confront the model to the CoGeNT data, tentatively interpreted as being due to DM, given our analysis of the best fit region in the $\sigma_n^0 - m_S$ plane. In particular, we show that, here too, the candidate may have the right relic density (see Fig. 1).² In Sec. III we present our exclusion limits based on the first data set released by the Xenon100 Collaboration [34]. We pay special attention to the impact of the uncertainties on the scintillation efficiency and argue that the exclusion limits are much weaker than those advocated in the Xenon100 article (see Fig. 3). Some other signatures and implications of a light scalar dark matter candidate are discussed in Sec. IV, in particular, the impact of the recent limits by Fermi-LAT on the gamma-ray flux from dwarf galaxies (see Table I), and the consequence for the search of an invisible Higgs at the LHC (see Fig. 5). Our results are summarized in the Conclusions, Sec. V.

¹A possible implementation is the inert doublet model (IDM), which is another very simple extension of the standard model (SM) with scalar DM [27–30]. See also [31,32].

²We include the recent data of the CDMS-II Collaboration [33] because it also points to a rather light DM candidate, although, with 2 events for an expected background of 0.8 ± 0.1 (stat) ± 0.2 (syst) events, the significance of this result is low.

II. CONFRONTATION TO THE COGENT DATA

We adopt the convention of [22], and consider just one real singlet scalar S , together with a Z_2 symmetry, $S \rightarrow -S$, to ensure its stability, so that the following renormalizable terms may be added to the SM Lagrangian:

$$\mathcal{L} \ni \frac{1}{2} \partial^\mu S \partial_\mu S - \frac{1}{2} \mu_S^2 S^2 - \frac{\lambda_S}{4} S^4 - \lambda_L H^\dagger H S^2, \quad (1)$$

where H is the standard model Higgs doublet, and the mass of S is given by

$$m_S^2 = \mu_S^2 + \lambda_L v^2, \quad (2)$$

with $v = 246$ GeV. Both annihilation into SM particles and scattering with nuclei are through the coupling λ_L to the Higgs particle h , respectively, in the s and t channels. Annihilation through the Higgs is S wave, and the cross section for scattering on nuclei, σ_n^0 , is purely of the SI type. For a DM candidate lighter than the Higgs, $m_S \ll m_h$, the ratio of the annihilation and scattering cross section depends only on m_S ,

$$\sum_f \frac{\sigma(SS \rightarrow \bar{f}f) v_{\text{rel}}}{\sigma(SN \rightarrow SN)} = \sum_f \frac{n_c m_f^2}{f^2 m_N^2 \mu_r^2} \frac{(m_S^2 - m_f^2)^{3/2}}{m_S}, \quad (3)$$

where $n_c = 3(1)$ for quarks (leptons), and $\mu_r = m_S m_N / (m_S + m_N)$ is the nucleon-DM reduced mass. The factor f parametrizes the Higgs to nucleons coupling, $f m_N \equiv \langle N | \sum_q m_q \bar{q} q | N \rangle = g_{hNN} v$, and we consider $0.2 \leq f \leq 0.4$ (see e.g. [36]).

Equation (3) shows that the mass of the DM candidate is fixed for a given relic abundance and SI scattering cross section [22,24–26]. In turn, direct detection experiments may determine both the SI cross section and the mass of the DM, modulo the astrophysical uncertainties regarding the local density and velocity distribution of the DM. *A priori* there is little chance that these constraints may be met by singlet scalar DM, but as Fig. 1 reveals, the model may be in agreement with CoGeNT—which is one of the main results of this article—or, as shown in [22,23], with DAMA. Since there is a gap between the CoGeNT and DAMA (with channeling) regions, that scalar DM agrees with CoGeNT does not trivially derive from the fact that it may agree with DAMA. We emphasize that this result, as for DAMA, is specific to a scalar particle with scalar couplings to SM fermions. For instance, annihilation through the Higgs portal would be P wave suppressed for a fermionic singlet DM candidate, and other interactions, as is the case for a light neutralino [37], are necessary to agree with the direct detection data (see also e.g. [38–41]).

The gap between CoGeNT and DAMA may be reduced, either assuming that channeling is less effective than what is advocated by the DAMA Collaboration (which has the effect of raising the DAMA region—but not reducing the tension with exclusion limits), or assuming that the CoGeNT excess is partially contaminated by some natural radioactivity (lowering the CoGeNT region) or a mixture

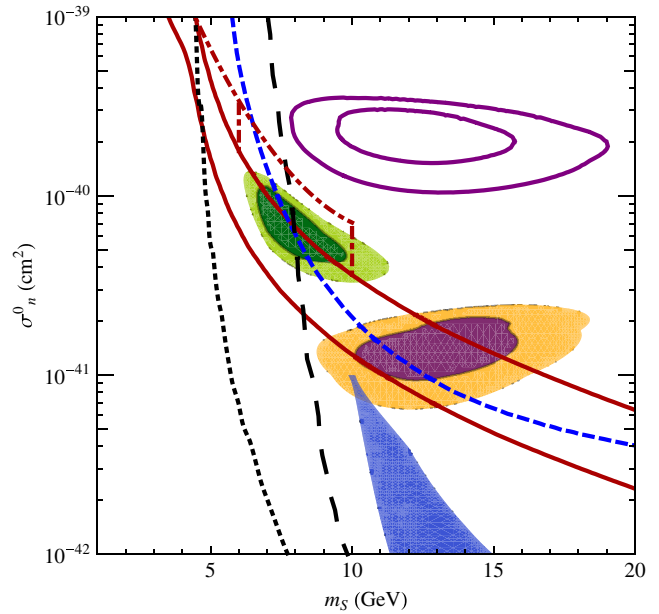


FIG. 1 (color online). SI cross section (σ_n^0) vs scalar singlet mass (m_S), for $\rho_{\text{DM}} = 0.3$ GeV/cm³ and a standard Maxwellian velocity distribution (with mean velocity 220 km/s and escape velocity $v_{\text{esc}} = 650$ km/s, see our conventions in [23]). The green region (light gray region centered on $m_S \approx 8$ GeV and $\sigma_n^0 \approx 7 \times 10^{-40}$ cm²) corresponds to CoGeNT (minimum χ^2 , with contours at 90% and 99.9% C.L.), for which we have assumed that the excess at low recoil energies is entirely due to DM (assuming a constant background contamination). The DAMA regions (goodness of fit, also at 90% and 99.9% C.L.) are given both with (purple/orange, darker gray region centered on $m_S \approx 13$ GeV and $\sigma_n^0 \approx 10^{-41}$ cm²) and without (purple, no fill) channeling. The blue region (triangular-shaped, gray region) corresponds to the CDMS-II two events, at 1σ , which we obtained following the procedure of [62]. The blue (short-dashed) line is the 90% C.L. exclusion limit from CDMS-Si [63]. The black dotted line is the 90% C.L. exclusion limit from the Xenon10 2009 data set, using their scintillation efficiency [64], as also considered in [62]. The long-dashed line is based on the same data but using instead the smaller scintillation efficiency advocated in [44] (central value, at 1σ the corresponding exclusion can be found in [39]). The brown lines (continuous) encompass the region predicted by the singlet scalar DM model corresponding to the WMAP range $0.094 \leq \Omega_{\text{DM}} h^2 \leq 0.129$, for $0.2 \leq f \leq 0.4$, for the QCD phase transition at a critical temperature $T_c = 150$ MeV (we have used micromegas to compute the relic abundances [65]). The dot-dashed brown lines illustrate the possible impact of having $T_c = 300$ MeV or $T_c = 500$ MeV (from left to right).

of both. One may also adjust the properties of the halo or the DAMA spectral data [39], but we have refrained from doing so.³

³Regarding the limitations of channeling and the possible overlap between DAMA and CoGeNT, we also refer to the recent [42,43], both works which have been released after completion of the present article.

Also, both regions are excluded by the most stringent limit set by Xenon10 (the dotted line in Fig. 1). However, if the scintillation efficiency—the measure of the fraction of energy from the recoiling nuclei that goes into scintillation light—is actually lower than that used by the collaboration (the long-dashed line in Fig. 1), as advocated in [44], there is a region of CoGeNT which may be consistent with all experimental constraints (and the singlet scalar DM candidate). The same issue arises regarding the more recent exclusion limits set by Xenon100, which apparently exclude the regions favored by DAMA and/or GoGeNT [34]. This conclusion is again very much dependent on the assumed properties of scintillation efficiency, an issue we dwell on in Sec. III.

Before we close this section, let us emphasize that, in the scenario we consider, the coupling λ_L to the Higgs must be fairly large to explain both the relic abundance and the direct detection data.⁴ For the same choice of parameters, $\mu_S \sim 100$ GeV, which implies fine-tuning of the parameters at the level of the percent, which is not unbearable in our opinion. Also there is no mechanism to naturally stabilize the mass of the scalar at a scale of a few GeV. Note however that, if neither CoGeNT nor DAMA could be fitted with $\mu_S^2 \sim 0$ at tree level, in the IDM at one loop, the DM mass and coupling ranges required by CoGeNT and/or DAMA may be compatible with dynamical electroweak symmetry breaking induced by the inert doublet [47].

III. XENON100 EXCLUSION LIMITS

Shortly after CoGeNT, the Xenon100 Collaboration released an analysis of their first data, collected over only 11.2 days [34]. The collaboration has found no event consistent with dark matter, and it has the world's best SI exclusion limits for dark matter mass $\lesssim 80$ GeV (Fig. 5 in [34]). More surprising, at first sight, is the limit set on lighter WIMPs, with mass $\lesssim 10$ GeV. In particular the CoGeNT and DAMA (with and without channeling) are excluded with 90% C.L.⁵ In this section, we present

⁴In the calculation of the relic abundance, the QCD phase transition is supposed to have taken place around ~ 150 MeV (see, for instance, [45]). Since typically $x_f = m_S/T_{fo} \approx 20$, for $m_S \approx 6$ GeV, for instance, the freeze-out temperature is $T_{fo} \approx 300$ MeV $\gg 150$ MeV and thus the QCD phase transition is irrelevant for the range of mass we consider. Otherwise, the QCD phase transition might increase the relic abundance by at most a factor of $O(2)$ (see for instance [46]). Such an increase could be compensated by an increase of λ_L by a factor of ~ 1.4 and this, in turn, would require a decrease of the parameter f by the same factor. For information, $m_h = 120$ GeV ($m_h = 180$ GeV), one typically requires $\lambda_L \approx -0.2$ (respectively, ≈ -0.45) for a DM candidate of mass $m_S \sim 8$ GeV. The possible effect of a QCD phase transition at a higher temperature is illustrated (brown dot-dashed lines) in Fig. 1.

⁵That something nonstandard is being done in this region may be appreciated by comparing Fig. 5 of [34] to the preliminary results presented at recent conferences (see for instance [48]) and is subject to discussion [49–51].

our own analysis of the low mass region, following the guidelines provided in Refs. [34,49–51], to which we refer for more details. For light dark matter candidates, the relevant features of the analysis of Xenon100 are as follows.

To discriminate dark matter (and neutron) collisions with Xe from electron and gamma events (a large source of background) the experiment relies on photoelectrons (PE) produced by scintillation (S1 signal). The relation between the mean number of PE, $n_{PE}(E_{nr})$, and the recoil energy E_{nr} (in keV) is given by the so-called scintillation efficiency (Leff). Which Leff to use, and how to extrapolate Leff at low E_{nr} (where no measurements of Leff exist) is an important issue [49]. The experimental situation on Leff is summarized in Fig. 1 of Ref. [50]. The exclusion limit set by Xenon100 in [34] is based on the best fit to current experimental data (LeffMed here), which gives $\text{Leff} \approx 0.12$ at small nuclei recoil energies E_{nr} . Furthermore Leff is set to zero for $E_{nr} \lesssim 1$ keV. A more conservative choice (LeffMin here, corresponding to a lower 90% C.L. fit to the data) gives a Leff which decreases monotonically with E_{nr} and vanishes at $E_{nr} \lesssim 1$ keV. The Zeplin experiment (also a Xe experiment) uses a different Leff, which is essentially zero below 6–7 keV (LeffZep here) [52].

In Fig. 2, following [50], we show the theoretical event rate (per kg and per day) for a mass = 10 GeV and $\sigma_{SI} = 10^{-41}$ cm² candidate, typical of the DAMA region. We use $v_{esc} = 544$ km s⁻¹ as the Xenon100 Collaboration. In the same figure, the size of the bins correspond to 0PE, 1PE, etc., given here for LeffMin. The threshold depends on the acceptance of the detector. For 3PE the acceptance is about 50%, and about 70% for 4PE (Fig. 3 of Ref. [34]). A standard analysis would give no event with 3PE or more. However, because of fluctuations (assumed to be Poissonian) in the number of PE produced, and because the event rate is exponentially rising at low E_{nr} (for elastic scattering), the rate is much larger at 3PE and 4PE, as shown by the histograms in Fig. 2, obtained by convolution of the theoretical rate with a Poisson distribution of mean $n_{PE}(E_{nr})$. For the sake of comparison we give the result of our calculation (black histogram), and that of Xenon100 (green/light gray histogram); see the figure in [50]. We have slightly more events at 3PE (hence we will have slightly stronger limits), but otherwise the agreement is good.

Our exclusion limits are shown in Fig. 3, where, in the left panel, we give the limits for a threshold at 3PE (consistent with Xenon100 [50]) and in the right panel the one for the more conservative choice of 4PE (consistent with Ref. [49]). From left to right, the exclusion limits correspond to LeffMed (short-dashed line), LeffMin (continuous line) and LeffZep (long-dashed line). For the latter, the cutoff in Leff is such that the effect of Poisson fluctuations from events at low E_{nr} is negligible, and one recovers the limit from a standard analysis.

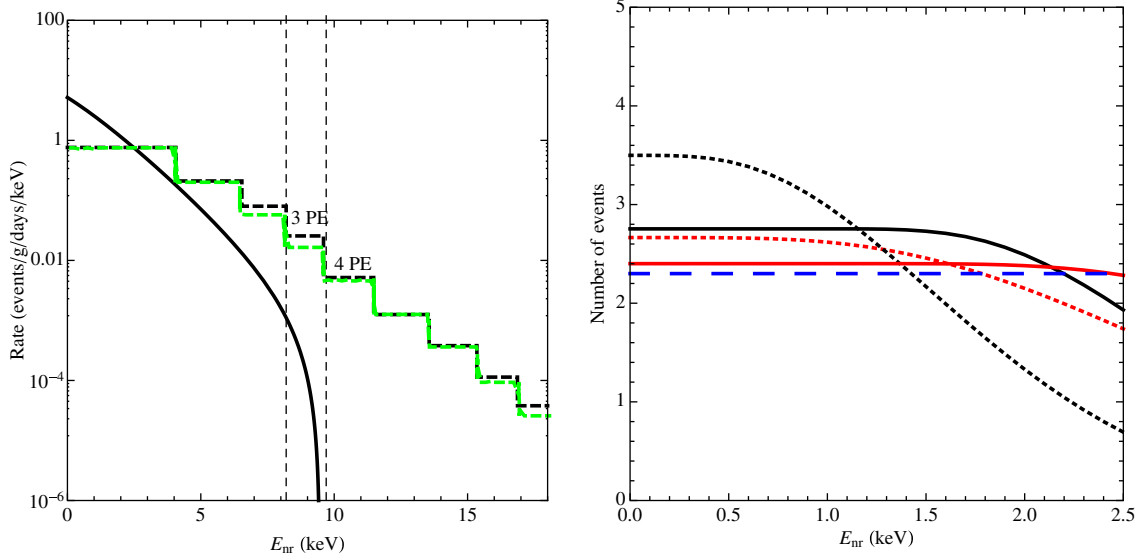


FIG. 2 (color online). Left panel: Effect of Poisson fluctuations on the expected signal (continuous curve) from a candidate with mass = 10 GeV and $\sigma_{SI} = 10^{-41} \text{ cm}^2$, assuming LeffMin (in green/light gray the Xenon100 bins, in black our bins—see text). The two vertical dashed lines correspond to the 3PE and 4PE thresholds. Right panel: Effects of changing the cutoff in the recoil energy (see text) on the number of events above 3PE (in black) and 4PE (in red/gray) for LeffMed (short-dashed lines), LeffMin (continuous lines), for a candidate of 6.5 GeV for LeffMed and of 7.5 GeV for LeffMin, both for $\sigma_{SI} = 10^{-40} \text{ cm}^2$. The horizontal long-dashed line corresponds to the 90% C.L. exclusion limit, which corresponds to 2.3 events according to Poisson statistics.

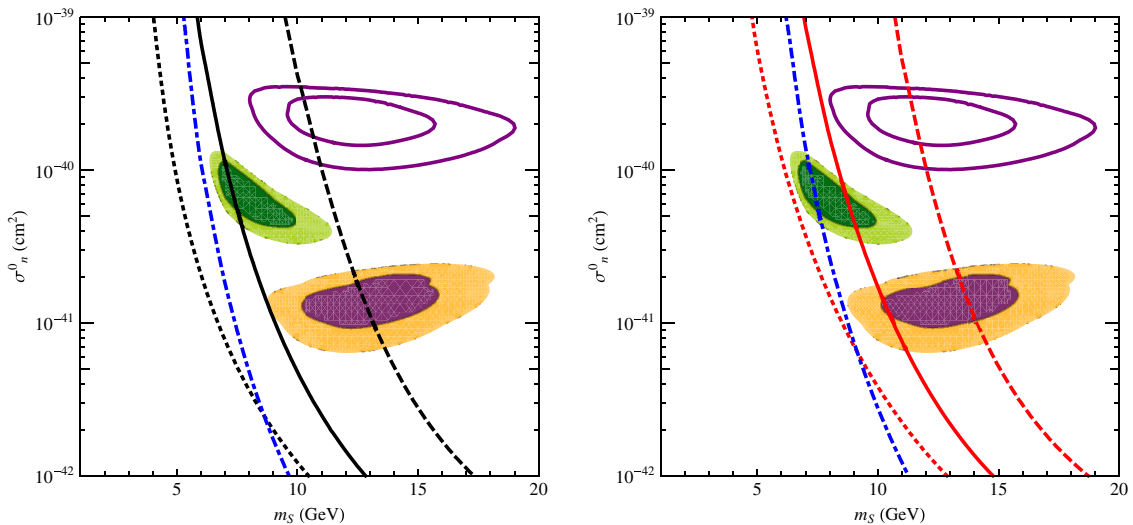


FIG. 3 (color online). Xenon100 exclusion limits with 90% C.L., with threshold at 3 PE (in black, left panel) or 4 PE (in red, right panel). The curves correspond, respectively, to the LeffMed (short-dashed lines), LeffMin (continuous lines) and LeffZep (long-dashed lines) scintillation efficiency—see text. For the sake of comparison, we have taken $v_{\text{esc}} = 544 \text{ km s}^{-1}$ like the Xenon100 Collaboration. The blue (dot-dashed) lines correspond to our predicted exclusion limit for Xenon100, using LeffMin and for an exposure of about 1 ton days, assuming zero event.

An important feature we observe is that a large fraction of the events at 3PE/4PE are associated with Poisson fluctuations from the small E_{nr} region, where the rate is very large, but less than 1PE is expected on average. As a result, if one increases the E_{nr} at which Leff vanishes, the number of low energy events that are lost (and which consequently do not contribute to higher energy

bins) quickly increases.⁶ This effect is illustrated in the right panel of Fig. 2, where we show the number of events above 3PE (respectively, 4PE) for candidates with

⁶This loss is the reason why the number of events in the first bin is about a factor 2 smaller than the theoretical number of events.

$\sigma_{\text{SI}} = 10^{-40} \text{ cm}^2$, both for LeffMed and LeffMin, but changing the cutoff E_{nr} at which they are assumed to vanish. The effect is most sensitive for LeffMed, where for a cutoff at $E_{\text{nr}} = 1 \text{ keV}$ the candidate is excluded at 90% C.L., while it is allowed if the cutoff is at $E_{\text{nr}} = 1.5 \text{ keV}$. In our exclusion limits we use the function LeffMed and LeffMin with a cutoff at $E_{\text{nr}} = 1 \text{ keV}$.

In our opinion, the method followed by the Xenon100 Collaboration to take into account Poisson fluctuations is *a priori* sound, but it is too sensitive (as discussed in [49–51]) to the choice of Leff at low E_{nr} to be safe. Here we would like to emphasize that not only the shape of Leff, but also the E_{nr} at which Leff is cut off, is a critical issue in setting exclusion limits.⁷

This being said, one must admit that there is a tension between the CoGeNT (and *a fortiori* DAMA) regions and the limits set by the Xenon100 experiment, and this with only limited exposure. Assuming that no events are seen in the data, we give in Fig. 3 our predicted exclusion limit of Xenon100, using LeffMin, for an exposure corresponding to 1 ton days (blue dot-dashed curve), as reported in [48]. This shows that, even for a conservative choice of Leff, most of the parameter space of CoGeNT and/or DAMA could be excluded.

IV. SOME OTHER SIGNATURES

A light scalar dark matter candidate coupled to the Higgs has potentially many other signatures or implications which have already been discussed elsewhere: a large flux of gamma rays from dark matter annihilations [11,22], a large flux of neutrinos from capture by the Sun, which may be constrained by Super-Kamiokande [14,54–56], or antiprotons and antideuterons in cosmic rays [6,57]. Here we first would like to point out that the annihilation and mass of the scalar singlet candidate we consider make it a very natural candidate to solve the primordial ${}^6\text{Li}$ problem, as is obvious from Fig. 3 in [58].

Furthermore, following a suggestion made in [39], we now tentatively confront the model to data on the gamma flux from dwarf galaxies recently released by the Fermi-LAT Collaboration [35]. The analysis in [35] gives, for various dwarf galaxies, the 95% C.L. limit on the total flux Φ of gamma rays (with energy between 100 MeV and 50 GeV) that may be produced through annihilation of dark matter. The published analysis, which is quite sophisticated, is limited to candidates with a mass larger than 10 GeV. However the spectrum of photons is quite similar for slightly lighter candidates (see Fig. 4), so we expect the

constraints to extrapolate smoothly for, say, a 6 GeV candidate. For the sake of illustration, we consider the limits from two representative dwarf galaxies, Draco and Ursa Minor [35]. In Table I, we give the predictions for the singlet scalar model for candidates with mass 6 and 10 GeV, assuming the Navarro-Frenk-White (NFW) [59] profile as used by the collaboration (see Table 4 of [35]), and for $\sigma v = 2.5 \times 10^{-26} \text{ cm}^3 \text{ s}^{-1}$.

For the limits on the gamma-ray flux from dwarf galaxies, we refer, in particular, to Fig. 2 of Ref. [35]. There are four plots in this figure, each corresponding to a specific branching ratio (BR) into $b\bar{b}$ and $\tau^+\tau^-$. For fixed BR, each of the plots gives the maximal allowed flux (in $\text{cm}^{-2} \text{ s}^{-1}$) at 95% C.L. as a function of the mass of the dark matter candidate, $10 \text{ GeV} \leq m_{\text{DM}} \leq 1 \text{ TeV}$, and for a selection of dwarf galaxies. For the case of the singlet scalar, a $m_s = 10 \text{ GeV}$ candidate annihilates dominantly into $b\bar{b}$ (the $\text{BR}_{\tau^+\tau^-} \approx 10\%$). In this case, it is a good approximation to refer to the limits as set in the top-left plot of Fig. 2 in [35], which corresponds to $\text{BR}_{b\bar{b}} = 100\%$ (see also Table I). From the plots of Fig. 2 in [35], we may infer that the $\text{BR}_{\tau^+\tau^-} \approx 10\%$ should give a limit on the flux that is $\mathcal{O}(10\%)$ stronger, at most. Unfortunately there are no limits for candidates lighter than 10 GeV but we nevertheless consider a candidate of mass 6 GeV which has $\text{BR}_{\tau^+\tau^-} \approx 20\%$ and $\text{BR}_{b\bar{b}} \approx 80\%$ making use of the bottom-left plot in Fig. 2 of [35]. If we naively extrapolate the exclusion limits curves down to 6 GeV, we obtain that the predicted fluxes are larger than the limits set by Fermi-

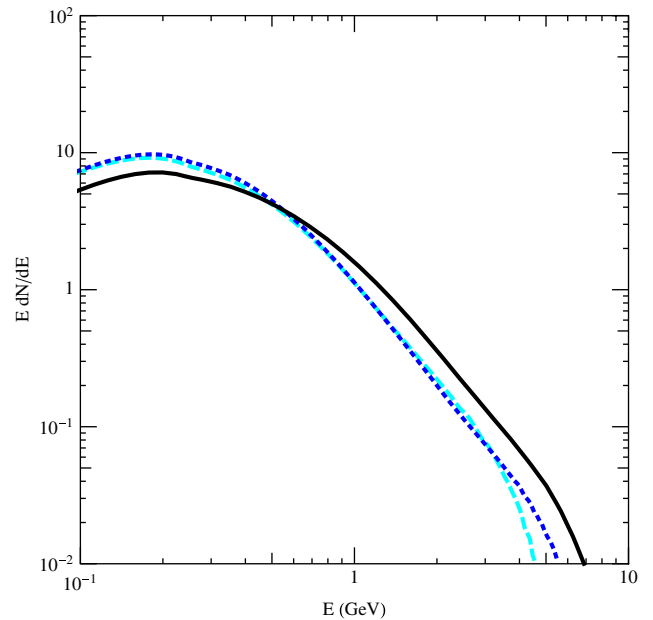


FIG. 4 (color online). Gamma-ray spectrum, $E dN/dE$, produced per annihilation for the case of a scalar singlet candidate of mass 6 GeV (blue, long-dashed line), 8 GeV (dark blue, short-dashed line) and 10 GeV (black, continuous line). The spectra have been produced with PYTHIA8.1 [66]. The branching ratios are as in Table I.

⁷After completion of the present work, the effect of changing Leff, both for Xenon10 and Xenon100, has been further discussed in [42]. In particular they give new exclusion limits for these experiments, based on a more conservative version of LeffMed. However they assume that there is no cutoff at lower recoil energies, a point which has been criticized in [53] with which we concur.

TABLE I. Comparison between the expected gamma-ray flux from a light scalar and the 95% C.L. limits given by the Fermi-LAT Collaboration, Fig. 2 in [35]. For the 10 GeV candidate the limits are extracted assuming annihilation into $b\bar{b}$ with a BR of 100%. The limits for the 6 GeV candidate are our extrapolations, assuming BR = 80% BR in $b\bar{b}$ and BR = 20% in $\tau^+\tau^-$.

m_S and BR	Ursa Minor		Draco	
	$\Phi_{\text{pred}} (\text{cm}^{-2} \text{s}^{-1})$	$\Phi_{\text{lim}}^{95\% \text{C.L.}} (\text{cm}^{-2} \text{s}^{-1})$	$\Phi_{\text{pred}} (\text{cm}^{-2} \text{s}^{-1})$	$\Phi_{\text{lim}}^{95\% \text{C.L.}} (\text{cm}^{-2} \text{s}^{-1})$
10 GeV				
BR($SS \rightarrow \tau^+\tau^-$) \approx 10%	8.5×10^{-10}	7.8×10^{-10}	1.6×10^{-9}	1.6×10^{-9}
BR($SS \rightarrow b\bar{b} + c\bar{c}$) \approx 90%				
6 GeV				
BR($SS \rightarrow \tau^+\tau^-$) \approx 20%	1.5×10^{-9}	1.0×10^{-9}	2.8×10^{-9}	1.7×10^{-9}
BR($SS \rightarrow b\bar{b} + c\bar{c}$) \approx 80%				

LAT. From the numbers given in Table I, we thus tentatively conclude that the scalar singlet model with a NFW profile may be excluded at 95% C.L. by data from dwarf galaxies. This result suggests that it would be most interesting to extend (more rigorously) the analysis of [35] to lighter WIMP candidates.

Last but not least, a light WIMP in the form of a scalar coupled to the Higgs would imply that the Higgs mostly decays into a pair of dark matter particles [22,25,26,60]. We would like to point out the fact that the DAMA and CoGeNT regions could be distinguished from a measurement of the invisible Higgs decay branching ratio. For $m_h = 180$ GeV the effect is striking: as Fig. 5 shows, taking into account the CDMS-Si limit and the WMAP region, the DAMA region gives $60\% \leq \text{BR} \leq 70\%$, while for the CoGeNT region, one has $75\% \leq \text{BR} \leq 90\%$. This difference is larger than the expected $\sim 10\%$ LHC sensitivity on the invisible branching ratio [61]. For $m_h = 120$ GeV, the difference is much reduced, because the invisible channel largely dominates the decay width: we

get $98\% \leq \text{BR} \leq 99\%$ and $\text{BR} \geq 99\%$ for DAMA and CoGeNT, respectively.

V. CONCLUSIONS

In this work, we have confronted a singlet scalar dark matter candidate interacting through the Higgs portal, to the recent direct detection data, most notably CoGeNT and Xenon100. As the properties of this dark matter candidate depend only on two parameters, i.e. m_S and λ_L , the relic density constraint allows one to express the direct detection cross section, σ_n^0 , as a function of m_S . The agreement with DAMA and/or CoGeNT is, if anything, intriguing. We provide in this article our own fits to the data which, to avoid cluttering, are shown in distinct figures. The most relevant constraints on the regions favored by CoGeNT and/or DAMA turned out to be those set by Xenon10 and CDMS-Si, as shown in Fig. 1. We have also studied in some detail the impact of (some of) the uncertainties on the scintillation efficiency, Leff , on the exclusion limits set by

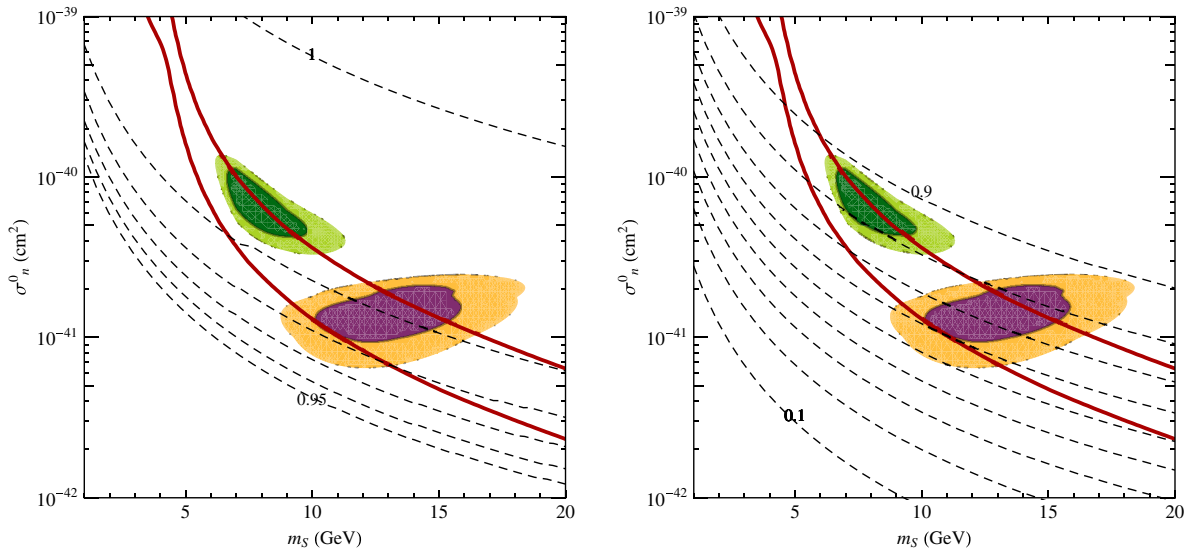


FIG. 5 (color online). These plots give, in the plane $\sigma_n^0 - m_S$, contour lines of constant Higgs invisible decay branching ratios, for the case of $m_h = 120$ GeV (left panel) and $m_h = 180$ GeV (right panel). In the latter case, the invisible BR are significantly distinct between the DAMA and CoGeNT regions.

Xenon100 [34]. As Fig. 3 shows, it is, in our opinion, too early to draw a definitive conclusion regarding the situation of CoGeNT and/or DAMA, as, depending of the choice of L_{eff} , their respective regions may or may not be excluded. Clearly more data, both in terms of brute exposure, but also on L_{eff} , will be necessary, as emphasized in some other recent works, to which we refer for more insight [42,43,49–51,53].

In this article, we also reemphasize the fact that a light DM particle may lead to a large flux of gamma rays and other messengers, some of which are summarized in Sec. IV. There we have also tentatively discussed the impact of the limits on the gamma-ray flux from dwarf galaxies set recently by the Fermi-LAT Collaboration [35]. In particular, in Table I we have compared the predicted flux of gamma rays from 10 GeV scalar candidate, to the 95% C.L. exclusion limits from two characteristic dwarf galaxies, assuming a NFW profile. We have furthermore naively extended the limits and have considered a lighter candidate, $m_s = 6$ GeV, than in [35]. In both cases, we have found that the limits are strong enough so as to constrain the singlet scalar model explanation for the DAMA and/or CoGeNT regions.

One last possible consequence of such a light scalar DM candidate, that we highlight in this work, is that the Higgs would essentially decay into an invisible channel. We have further discussed this possibility in the light of the two distinct (according to our analysis) regions corresponding to DAMA and CoGeNT. We have pointed out that, provided that the Higgs is heavy enough to be able to decay in weak boson pairs, the difference in the invisible branching ratios corresponding to these regions might be measurable at the LHC.

ACKNOWLEDGMENTS

We thank Martin Casier, Juan Collar, Jan Conrad, Karsten Jedamzik, and Thomas Schwetz for useful discussions. Our work is supported by the FNRS-FRS, the IISN, and the Belgian Science Policy (IAP VI-11).

Note added in proof.—The constraints on light WIMPs from the limits on the flux of gamma rays emitted by dwarf galaxies anticipated in the present article (see Table I) are consistent with preliminary analyses presented by the Fermi-LAT Collaboration at the 8th International Workshop Identification of Dark Matter 2010 (IDM 2010) [67].

-
- [1] C. E. Aalseth *et al.* (CoGeNT Collaboration), [arXiv:1002.4703](#).
 - [2] J. P. Ralston, [arXiv:1006.5255](#).
 - [3] R. Bernabei *et al.* (DAMA Collaboration), *Eur. Phys. J. C* **56**, 333 (2008).
 - [4] A. K. Drukier, K. Freese, and D. N. Spergel, *Phys. Rev. D* **33**, 3495 (1986).
 - [5] K. Freese, J. A. Frieman, and A. Gould, *Phys. Rev. D* **37**, 3388 (1988).
 - [6] A. Bottino, F. Donato, N. Fornengo, and S. Scopel, *Phys. Rev. D* **78**, 083520 (2008).
 - [7] R. Foot, *Phys. Rev. D* **78**, 043529 (2008).
 - [8] S. Chang, A. Pierce, and N. Weiner, *Phys. Rev. D* **79**, 115011 (2009).
 - [9] M. Y. Khlopov, [arXiv:0806.3581](#).
 - [10] R. Bernabei *et al.* (DAMA Collaboration), *Mod. Phys. Lett. A* **23**, 2125 (2008).
 - [11] J. L. Feng, J. Kumar, and L. E. Strigari, *Phys. Lett. B* **670**, 37 (2008).
 - [12] E. Masso, S. Mohanty, and S. Rao, *Phys. Rev. D* **80**, 036009 (2009).
 - [13] F. Petriello and K. M. Zurek, *J. High Energy Phys.* **09** (2008) 047.
 - [14] C. Savage, G. Gelmini, P. Gondolo, and K. Freese, *J. Cosmol. Astropart. Phys.* **04** (2009) 010.
 - [15] S. Chang, G. D. Kribs, D. Tucker-Smith, and N. Weiner, *Phys. Rev. D* **79**, 043513 (2009).
 - [16] E. Dudas, S. Lavignac, and J. Parmentier, *Nucl. Phys.* **B808**, 237 (2009).
 - [17] Y. Cui, D. E. Morrissey, D. Poland, and L. Randall, *J. High Energy Phys.* **05** (2009) 076.
 - [18] J. March-Russell, C. McCabe, and M. McCullough, *J. High Energy Phys.* **05** (2009) 071.
 - [19] M. Fairbairn and T. Schwetz, *J. Cosmol. Astropart. Phys.* **01** (2009) 037.
 - [20] A. Bandyopadhyay, S. Chakraborty, A. Ghosal, and D. Majumdar, [arXiv:1003.0809](#).
 - [21] F.-S. Ling, [arXiv:0911.2321](#) [*Phys. Rev. D* (to be published)].
 - [22] S. Andreas, T. Hambye, and M. H. G. Tytgat, *J. Cosmol. Astropart. Phys.* **10** (2008) 034.
 - [23] C. Arina, F.-S. Ling, and M. H. G. Tytgat, *J. Cosmol. Astropart. Phys.* **10** (2009) 018.
 - [24] J. McDonald, *Phys. Rev. D* **50**, 3637 (1994).
 - [25] C. P. Burgess, M. Pospelov, and T. ter Veldhuis, *Nucl. Phys.* **B619**, 709 (2001).
 - [26] V. Barger, P. Langacker, M. McCaskey, M. J. Ramsey-Musolf, and G. Shaughnessy, *Phys. Rev. D* **77**, 035005 (2008).
 - [27] N. G. Deshpande and E. Ma, *Phys. Rev. D* **18**, 2574 (1978).
 - [28] R. Barbieri, L. J. Hall, and V. S. Rychkov, *Phys. Rev. D* **74**, 015007 (2006).
 - [29] E. Ma, *Phys. Rev. D* **73**, 077301 (2006).
 - [30] L. Lopez Honorez, E. Nezri, J. F. Oliver, and M. H. G. Tytgat, *J. Cosmol. Astropart. Phys.* **02** (2007) 028.
 - [31] M. Kadastik, K. Kannike, and M. Raidal, *Phys. Rev. D* **80**, 085020 (2009); **81**, 029903(E) (2010).

- [32] M. Kadastik, K. Kannike, and M. Raidal, *Phys. Rev. D* **81**, 015002 (2010).
- [33] Z. Ahmed *et al.* (The CDMS-II Collaboration), [arXiv:0912.3592](https://arxiv.org/abs/0912.3592).
- [34] E. Aprile *et al.* (XENON100 Collaboration), [arXiv:1005.0380](https://arxiv.org/abs/1005.0380).
- [35] A. A. Abdo *et al.*, *Astrophys. J.* **712**, 147 (2010).
- [36] J. Gasser, H. Leutwyler, and M. E. Sainio, *Phys. Lett. B* **253**, 260 (1991).
- [37] A. Bottino, F. Donato, N. Fornengo, and S. Scopel, *Phys. Rev. D* **77**, 015002 (2008).
- [38] Y. G. Kim and S. Shin, *J. High Energy Phys.* **05** (2009) 036.
- [39] A. L. Fitzpatrick, D. Hooper, and K. M. Zurek, *Phys. Rev. D* **81**, 115005 (2010).
- [40] E. Kuflik, A. Pierce, and K. M. Zurek, *Phys. Rev. D* **81**, 111701 (2010).
- [41] D. Feldman, Z. Liu, and P. Nath, *Phys. Rev. D* **81**, 117701 (2010).
- [42] C. Savage, G. Gelmini, P. Gondolo, and K. Freese, [arXiv:1006.0972](https://arxiv.org/abs/1006.0972).
- [43] D. Hooper, J. I. Collar, J. Hall, and D. McKinsey, [arXiv:1007.1005](https://arxiv.org/abs/1007.1005).
- [44] A. Manzur *et al.*, *Phys. Rev. C* **81**, 025808 (2010).
- [45] L. McLerran, in *Proceedings of the 8th Workshop on Continuous Advances in QCD*, edited by M. Peloso (World Scientific, Hackensack, 2008).
- [46] A. Bottino, F. Donato, N. Fornengo, and S. Scopel, *Phys. Rev. D* **68**, 043506 (2003).
- [47] T. Hambye and M. H. G. Tytgat, *Phys. Lett. B* **659**, 651 (2008).
- [48] L. Aprile's, in Proceedings of the WONDER Workshop, 2010 (to be published).
- [49] J. I. Collar and D. N. McKinsey, [arXiv:1005.0838](https://arxiv.org/abs/1005.0838).
- [50] Xenon100 Collaboration, [arXiv:1005.2615](https://arxiv.org/abs/1005.2615).
- [51] J. I. Collar and D. N. McKinsey, [arXiv:1005.3723](https://arxiv.org/abs/1005.3723).
- [52] V. N. Lebedenko *et al.*, *Phys. Rev. D* **80**, 052010 (2009).
- [53] J. I. Collar, [arXiv:1006.2031](https://arxiv.org/abs/1006.2031).
- [54] C. Savage, K. Freese, P. Gondolo, and D. Spolyar, *J. Cosmol. Astropart. Phys.* **09** (2009) 036.
- [55] S. Andreas, M. H. G. Tytgat, and Q. Swillens, *J. Cosmol. Astropart. Phys.* **04** (2009) 004.
- [56] J. L. Feng, J. Kumar, J. Learned, and L. E. Strigari, *J. Cosmol. Astropart. Phys.* **01** (2009) 032.
- [57] E. Nezri, M. H. G. Tytgat, and G. Vertongen, *J. Cosmol. Astropart. Phys.* **04** (2009) 014.
- [58] K. Jedamzik and M. Pospelov, *New J. Phys.* **11**, 105028 (2009).
- [59] Julio F. Navarro, Carlos S. Frenk, and Simon D. M. White, *Astrophys. J.* **462**, 563 (1996).
- [60] X.-G. He, T. Li, X.-Q. Li, J. Tandean, and H.-C. Tsai, *Phys. Lett. B* **688**, 332 (2010).
- [61] O. J. P. Eboli and D. Zeppenfeld, *Phys. Lett. B* **495**, 147 (2000).
- [62] J. Kopp, T. Schwetz, and J. Zupan, *J. Cosmol. Astropart. Phys.* **02** (2010) 014.
- [63] D. S. Akerib *et al.* (CDMS Collaboration), *Phys. Rev. Lett.* **96**, 011302 (2006).
- [64] J. Angle *et al.* (XENON10 Collaboration), *Phys. Rev. D* **80**, 115005 (2009).
- [65] G. Belanger, F. Boudjema, A. Pukhov, and A. Semenov, *Comput. Phys. Commun.* **176**, 367 (2007).
- [66] T. Sjostrand, S. Mrenna, and P. Z. Skands, *Comput. Phys. Commun.* **178**, 852 (2008).
- [67] J. Conrad and M. Llana Garde, in Proceedings of the 8th International Workshop Identification of Dark Matter 2010 (to be published).